# Measurement of the Rayleigh-Taylor Instability in Targets Driven by Optically Smoothed Laser Beams

M. Desselberger and O. Willi
*Imperial College of Science, Technology and Medicine, London, United Kingdom*

M. Savage and M. J. Lamb
*The Queen's University of Belfast, Belfast, United Kingdom*
(Received 18 June 1990)

Growth rates of the Rayleigh-Taylor instability were measured in targets with imposed sinusoidal modulations irradiated by optically smoothed 0.53-$\mu$m laser beams. A hybrid optical smoothing technique utilizing induced-spatial-incoherence and random-phase-plate technology was used for the first time. The wave-number dependence and the nonlinear behavior of Rayleigh-Taylor growth were investigated by using targets with a range of modulation periodicities and depths. The results are compared to 2D hydrodynamic-code simulations.

PACS numbers: 52.40.Nk, 52.35.Py, 52.65.+z

The Rayleigh-Taylor (RT) hydrodynamic instability occurs in any accelerating fluid system in which the density and pressure gradients are of opposite sign. In the case of inertial-confinement-fusion (ICF) experiments, the hot, low-density ablating plasma accelerates a cooler, more dense part of the target and is thus susceptible to the RT instability. In an ICF implosion small imperfections in the target manufacture or intensity nonuniformities present in the laser irradiation may initiate RT growth sufficient to disrupt the target symmetry to an unacceptable degree. Thus efforts to reduce the RT growth rate in laser-irradiated targets are of immense importance to ICF and a precise understanding of the growth process is essential.

The RT growth rate has been measured experimentally in laser-accelerated foil targets with sinusoidal modulations.[1] The targets were, however, driven by coherent laser beams with large intensity variations across the beam profiles. Recent experimental efforts have concentrated on improving the irradiation uniformity by utilizing either radiative drive[2] or smoothed infrared (1 $\mu$m) drive illumination[3] using the induced-spatial-incoherence (ISI) technique.[4] At present, the trend in ICF is towards shorter laser wavelengths, where a reduction of target preheat has been observed and improved RT instability stabilization is expected.[5] This Letter reports on the results of a recent experiment in which thin foil targets were accelerated with uniform green (0.53 $\mu$m) laser illumination. Uniformity of the laser-beam profiles was achieved by a novel hybrid optical smoothing technique which consisted of an induced-spatial-incoherence and random-phase-plate[4,6] (RPP) array. Experimental growth rates and results of computer simulations are reported. The previously reported[3] anomalously small growth rate for 50-$\mu$m-modulation-periodicity targets with ISI irradiation was not observed in our experiment.

Six frequency-doubled green (0.53 $\mu$m) beams, arranged in a hexagonal cluster with a cone angle of 13°, were focused onto thin foil targets with $f/10$ lenses. The six superimposed 1.76-ns (FWHM) beams generated a smooth, flat-topped spatial intensity profile providing uniform acceleration across the target surface. The irradiance was kept constant at $1.5\times10^{14}$ W cm$^{-2}$ throughout the experiment to allow direct comparison of the results for different target specifications. The laser beams were smoothed by a hybrid scheme consisting of a combination of ISI and RPP arrays. The ISI was generated using a broadband oscillator ($\Delta\omega/\omega=0.1\%$) and a $6\times6$ echelon array to produce 36 independent beamlets. In addition to profile smoothing, the RPP's (placed immediately in front of the six lenses) have the effect of increasing the far-field focal-spot size (to 335 $\mu$m diameter) and of increasing the depth of focus. The RPP-ISI combination produces an RPP-type profile (with only short-scale-length nonuniformities) which is smoothed by the ISI over many coherence times. An x-ray pinhole camera, filtered for an x-ray energy band between 0.84 and 1.63 keV, was used to monitor the uniformity and size of the focal spot produced by the drive beams. Intensity variations of less than 1% (calculated using a 2D weighted averaging procedure) were seen over a spatial scale length of 10 $\mu$m. A time-integrated x-ray image may be significantly smoothed by the motion of the plasma over several nanoseconds. For this reason the intensity uniformity in the visible was also monitored by imaging a fraction of one of the drive beams. Again, a 2D weighted average of the intensity variations was calculated and showed $\Delta I/I\simeq1\%$ over a 10-$\mu$m spatial scale. Further, the focal-spot intensity profile was computed, for our experimental conditions, using an interference code. A detailed analysis of the degree of uniformity ($\Delta I/I$) and of the spatial frequency structure in the computed and experimentally determined intensity profiles was made and showed good agreement.[7] The degree of uniformity

 

achieved ensured that any RT growth due to intensity nonuniformities in the drive beams was small and thus does not influence the growth-rate measurements.

The targets consisted of low-density (0.9 g/cm$^3$) ($CH_2$) plastic approximately 16 $\mu$m thick with sinusoidal modulations of periodicity 30, 50, 70, and 100 $\mu$m. Modulation depths between 1.8 and 4.6 $\mu$m were investigated, with the modulations always facing the drive beams. The accelerated targets were backlit with a Mg backlighter source which was generated by a separate green laser beam 2.5 ns in duration. The transmitted fraction of the x rays produced by the backlighter source was imaged, through a narrow-band (0.8 keV) CH and Al ($K$ edge) filter, onto a streak camera by means of a 17-$\mu$m pinhole. The modulation transfer function (MTF) of this imaging system was measured independently, giving values of 0.33, 0.73, 0.95, and 0.97 for 30-, 50-, 70-, and 100-$\mu$m spatial scale lengths, respectively. The backlighter spectrum was measured using a time-integrated crystal spectrometer with filtering identical to that used in front of the streak camera. This showed that the backlighter x-ray emission was contained principally ($> 85\%$) in the Mg $He_\alpha$ (1.35 keV) and Ly-$\alpha$ (1.47 keV) transitions. Control experiments with only the drive irradiation (to determine the intensity level of target self-emission) and with backlighter illumination only (for calibration purposes) were conducted. In addition to the transmission radiographs, streaked edge-on radiographs of unmodulated targets were recorded to obtain the target acceleration and to monitor target decompression ($< 20\%$ over 2.3 ns).

Computer simulations of the experiment were performed using the 2D Eulerian hydrodynamics code POLLUX which has been extensively tested under various conditions and is described in detail elsewhere.[8] The code was modified to incorporate the sinusoidal target surface modulations and matched to the experimental conditions by varying the absorbed (green) irradiance until the inertial motion measured in the experiment was reproduced in the simulations. The absorbed irradiance was chosen as the variable parameter, since it is the least accurately characterized experimental quantity due to lateral-energy-transport effects. It was found that approximately 50% of the measured energy was absorbed and reproduced the experimentally determined inertial motion. This value is comparable to previous measurements under similar conditions.[2] The simulated and observed growth time histories were very similar and were not strictly exponential. This is due largely to the time-dependent drive intensity (modeled in the simulations) but may, at late times, also be due to possible saturation effects.

Figure 1 shows two time-resolved x-ray radiographs for targets with modulation periodicities of 100 and 50 $\mu$m, respectively. An edge-on radiograph from which a plot of target displacement (and thus acceleration) versus time could be obtained is shown in Fig. 2. Microdensitometry of streak records such as those shown in Fig. 1 yielded quantitative measures of the x-ray contrast levels (and thus ripple amplitudes) observed at different times. Both the initial modulation depth and the instability growth rate were then deduced from exponential curves fitted to these data. The growth rates measured in this way are plotted in Fig. 3 as fractions of their classically predicted values, the errors representing the spread in the amplitude of different modulations on the target evi-

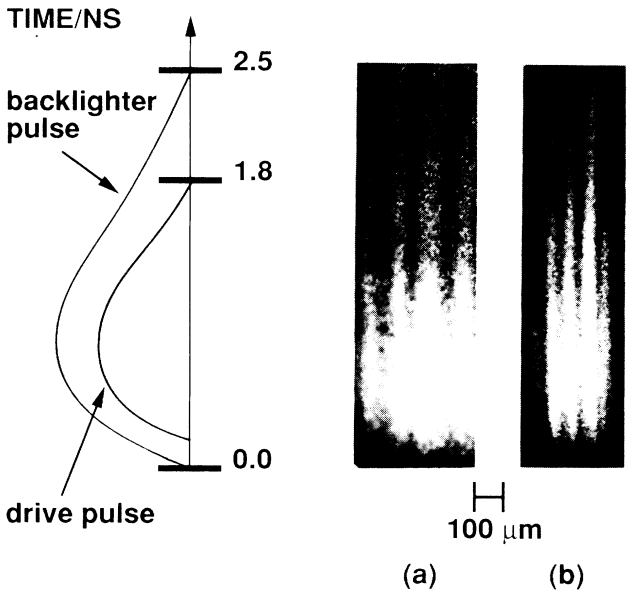


FIG. 1. Examples of time-resolved x-ray radiographs of ($CH_2$) targets 16 $\mu$m thick, with a 4.5-$\mu$m modulation depth and (a) 100-$\mu$m and (b) 50-$\mu$m modulation periodicity. The targets were irradiated with a laser wavelength of 0.53 $\mu$m and an irradiance of $1.5\times10^{14}$ W cm$^{-2}$.

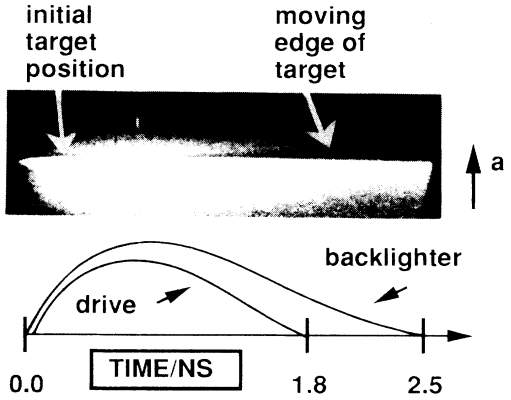


FIG. 2. Edge-on streak radiograph of an accelerated target. An average target acceleration of $6.6\times10^{15}$ W cm$^{-2}$ (for the period from 400 to 1700 ps after the start of the drive pulse) was derived from this observation for an irradiance of $1.5\times10^{14}$ W cm$^{-2}$.

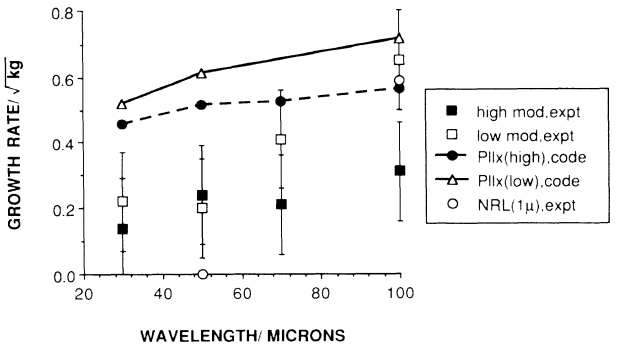


FIG. 3. Measured RT growth rates presented as fractions of the classical growth rate $(kg)^{1/2}$ (where $k$ is the modulation wave number and $g$ is the acceleration) for both high- (4.5 $\mu$m) and low- (2.6 $\mu$m for 30- and 50-$\mu$m periodicity; 1.8 $\mu$m for 70- and 100-$\mu$m periodicity) modulation-depth targets. Also shown are POLLUX ($\lambda = 0.5$ $\mu$m) results for 1.8-$\mu$m (low) and 4.5-$\mu$m (high) modulation-depth targets and experimental results from Ref. 3, where the error bars are omitted for clarity.

dent at late times. The measured initial ($t = 0$) modulation depths were convolved with the MTF of the imaging system and compared to the known initial modulation depths (accurately measured by microscopy before the experiment). No significant discrepancy was found (error less than 0.4 $\mu$m). Further, no growth-rate analysis was carried out during the initial period in which the shock passes through the target. In this time, the growth is not due to the RT instability but due to the shock-driven Richtmeyer-Meshkov instability and is quadratic in time.[9] The shock transit time was estimated to be 300 ps for our conditions using the one-dimensional Lagrangian hydrodynamics code MEDUSA.[10] The x-ray contrast profile at shock breakthrough is indicative of the initial ($t = 0$) drive-beam spatial profile and thus serves as an additional monitor of uniformity.

The most striking result from Fig. 3 is that the 50-$\mu$m-periodicity targets clearly exhibited growth, where a previous experiment also utilizing ISI (under low irradiance conditions $\simeq 5\times 10^{12}$ W cm$^{-2}$ and using infrared light)[3] found none.

It is also evident from Fig. 3 that the lower-modulation-depth targets tend to exhibit faster growth than the ones with deeper modulations, indicating that the growth is at least partially taking place in the nonlinear regime. The observed onset of nonlinear growth is consistent with a criterion developed in Ref. 11, which states that growth is expected to be linear for $A/\lambda \lesssim 0.05$, where $A$ is the initial modulation depth and $\lambda$ the modulation periodicity. From the transmission radiographs it is evident that the ripples maintain an approximately sinusoidal structure and are not observed to narrow significantly (as would be expected during bubble and spike formation late in the nonlinear regime of growth). This is because the nonlinear growth has not progressed sufficiently over the period of our observations (2–3 $e$ folds). A recent numerical study[12] predicts sinusoidal ripple structure up to $A/\lambda \simeq 0.4$, well into the nonlinear regime of growth. This corresponds to 3 $e$ folds of growth for an $A = 2$ $\mu$m, $\lambda = 100$ $\mu$m target. However, in the regime where $A/\lambda \gtrsim 0.5$, numerous simulations predict intense spike and bubble formation. Recently, this has been observed experimentally with radiative drive.[2]

Also plotted in Fig. 3 are the measured growth rates of the NRL experiment[3] and those predicted by the POLLUX simulations (for both high and low modulation depths). Several points arise. First, the qualitative wavelength dependence of the observed growth rates is in fair agreement with the dependence predicted by the simulations; growth was observed at all modulation periodicities including 50 $\mu$m. Second, the growth rates predicted by the simulations are (except for two points) outside the error bars and greater than the observed rates. This must not be purely due to the nonlinearity of the growth, but may in part be due to radiation transport effects not included in the modeling. These would, in principle, reduce the growth rate. Other omitted or inaccurately modeled parameters include ion viscosity, equation of state, and magnetic-field generation. The excitation of higher-order modes, described in Ref. 13, also reduces the growth rate of the fundamental. To investigate the extent of such higher-order contributions to the growth of the instability, the spatial frequency spectra of the x-ray radiographs were analyzed by Fourier decomposition. The 100-$\mu$m-periodicity targets exhibited second-harmonic Fourier amplitudes of up to 20% of the fundamental after 2 ns of growth (with lower values for the third and fourth harmonics). Second-harmonic growth was not clearly observed in the case of the 50-$\mu$m targets, where only the fundamental mode was found to have a significant Fourier component. The resolution of the imaging system was insufficient to conclusively detect growth at wavelengths shorter than 25 $\mu$m. However, because of increased convective stabilization at shorter wavelengths, we expect growth below this value to be severely suppressed under our conditions.

The growth rates predicted by the simulations were found to be well approximated by the functional form $\alpha A(kg)^{1/2} - \beta k V_a$, where $A$ is the Attwood number ($A \simeq 1$ for the laser-ablative case), $k$ is the wave vector, $g$ is the acceleration, and $V_a$ is the ablation velocity ($V_a \simeq 2$ $\mu$m/ns, from the simulations). The coefficient $\alpha$ represents the degree of density-gradient stabilization and is found in Ref. 14 to be $\alpha = (1+kL)^{-1/2}$, where $L$ is the density scale length at the ablation front. From the simulations $L \simeq 2$ $\mu$m, so $\alpha$ is approximately 0.9 for our conditions; $\beta$, the coefficient of convective stabilization, was determined from Ref. 15 and takes a value of about 3.0. With these values agreement between the formula and the POLLUX predictions is within about 10%.

In summary, the growth rate of the RT instability was measured on corrugated targets with modulation periodicities of 30–100 $\mu$m which were irradiated with ISI +RPP hybrid illumination. Observed growth rates were in the range of approximately 0.25–0.5 of the classically predicted values and lower-modulation-depth targets exhibited faster growth than high-modulation targets, indicating the nonlinearity of the process. Although nonlinearity was observed, our observations did not extend into the regime where intense spike and bubble formation occurs. This regime could be studied by increasing either the drive intensity or the drive duration. Further, the measured rates were generally lower than those predicted by the hydrodynamic-code simulations and by the formula described; it seems that competing higher-harmonic processes at least partly explain this. Further work is needed on the characterization of the nonlinearity of the instability. In particular, low-modulation-depth targets initiating growth well inside the linear regime ($A/\lambda < 0.01$) are needed to properly experimentally characterize the growth in this region with smoothed laser beams.

We wish to thank the Central Laser Facility's laser division staff, especially C. Danson and the Target Preparation staff for their assistance. We also thank Dr. R. Evans for his assistance with the simulations. This work was supported by the Science and Engineering Research Council.

[1]A. Cole, J. D. Kilkenny, P. T. Rumsby, R. G. Evans, C. J. Hooker, and M. H. Key, Nature (London) **299**, 329 (1982).

[2]J. D. Kilkenny, Bull. Am. Phys. Soc. **34**, 2040 (1989).

[3]J. Grun *et al.*, Phys. Rev. Lett. **58**, 2672 (1987).

[4]R. H. Lehmberg and S. P. Obenschain, Opt. Commun. **46**, 27 (1983).

[5]M. H. Emery, J. H. Gardner, and S. E. Bodner, Phys. Rev. Lett. **57**, 703 (1986).

[6]Y. Kato and K. Mima, Phys. Rev. Lett. **53**, 1057 (1984).

[7]M. Desselberger and O. Willi (to be published).

[8]G. J. Pert, J. Comput. Phys. **43**, 111 (1981).

[9]D. H. Munro, Phys. Fluids B **1**, 134 (1989).

[10]J. Christiansen, D. Ashby, and K. Roberts, Comput. Phys. Commun. **7**, 271 (1974).

[11]D. L. Youngs, M. J. Henshaw, and G. J. Pert, Plasma Phys. Controlled Fusion **29**, 405 (1987).

[12]K. O. Mikaelian, Phys. Rev. A **42**, 4944 (1990).

[13]S. W. Haan, Phys. Rev. A **39**, 5812 (1989).

[14]D. H. Munro, Phys. Rev. A **38**, 1433 (1988).

[15]H. Takabe, K. Mima, L. Montierth, and R. L. Morse, Phys. Fluids **28**, 3676 (1985).

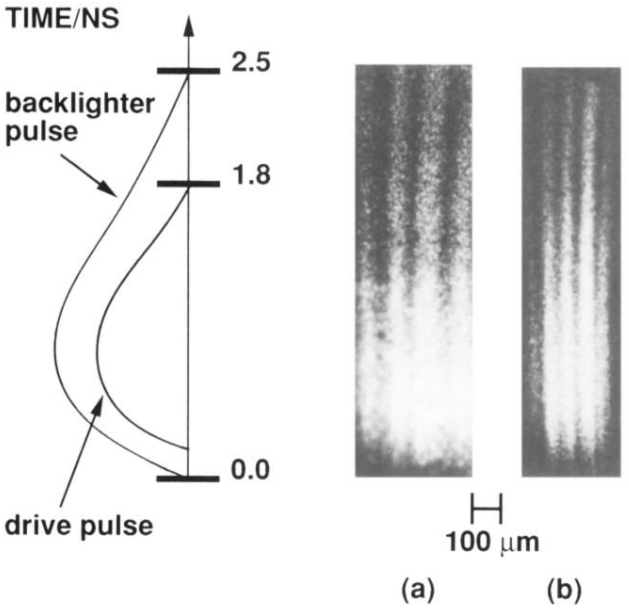


FIG. 1. Examples of time-resolved x-ray radiographs of ($CH_2$) targets 16 $\mu$m thick, with a 4.5-$\mu$m modulation depth and (a) 100-$\mu$m and (b) 50-$\mu$m modulation periodicity. The targets were irradiated with a laser wavelength of 0.53 $\mu$m and an irradiance of $1.5\times10^{14}$ W cm$^{-2}$.

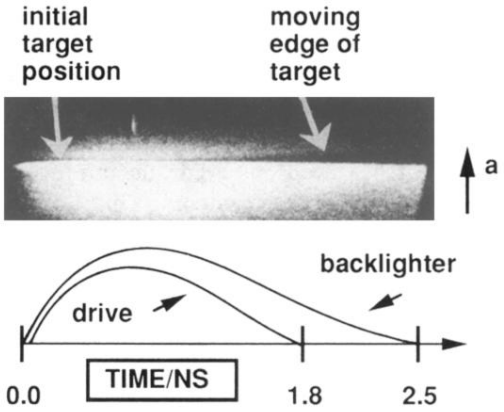


FIG. 2. Edge-on streak radiograph of an accelerated target. An average target acceleration of $6.6\times10^{15}\,\mathrm{W\,cm^{-2}}$ (for the period from 400 to 1700 ps after the start of the drive pulse) was derived from this observation for an irradiance of $1.5\times10^{14}\,\mathrm{W\,cm^{-2}}$.